Single Fiber Fragmentation Test for Evaluating Fiber-Matrix Interfacial Strength: Testing Procedure and Its Improvements

Bentang Arief Budiman[1,*], Djoko Suharto[1], Kikuo Kishimoto[2], Farid Triawan[2], Kosuke Takahashi[3], Kazuaki Inaba[2]

[1]Mechanical Engineering Department, Faculty of Mechanical and Aerospace Engineering, Institut Teknologi Bandung, Jl Ganesha 10 Bandung 40132, Indonesia

[2]Department of Transdisciplinary Science and Engineering, Tokyo Institute of Technology, 2-12-1 I6-10, Ookayama, Meguro-ku, Tokyo 152-8552, Japan

[3]Division of Mechanical and Aerospace Engineering, Hokkaido University, N13, W8, Kita-ku, Sapporo, Hokkaido, 060-8628, Japan

*Email: bentang@ftmd.itb.ac.id

Abstract

This paper exhibits single fiber fragmentation test (SFFT) method for evaluating interfacial strength between fiber and matrix composite. Two types of SFFT specimens i.e. with and without an agent material for strengthening the interface were used for the tests. A specimen manufacturing was conducted precisely in order to assure a uniformly interfacial strength. The specimens were imposed by a tensile force using micro-tensile test machine until the process of fragmentation was on saturated condition. The fragmented lengths were then measured and analyzed further by using Kelly-Tyson model in order to obtain the interfacial strength. Testing results showed that SFFT can differentiate interfacial strength from two types of the specimens. Several SFFT weaknesses including improving methods and their analyses previously proposed were also discussed.

Keywords: Single fiber fragmentation test, fiber-matrix interface, interfacial strength, composite failure.

Introduction

The main problem in utilizing a composite based on fiber and matrix as load-bearing structures is a complexity in predicting a composite failure [1-3]. The failure is started from cracks occur on the fiber, matrix, and interface which are then integrated and propagated [4]. Not like mechanical properties of fiber or matrix which has been researched comprehensively, interfacial properties have not obtained special attention even though it could bring a significant contribution to the composite failure [5].

Figure 1 shows characteristics of fiber surface which can affect interfacial properties particularly interfacial strength (t_o). For evaluating optimal t_o, each surface characteristic has to be controlled properly in fiber manufacturing. The fiber surface is always coated by an agent-material to strengthen the t_o on sizing process [6-9]. In other hand, porosities which can cause micro cracks have to be avoided.
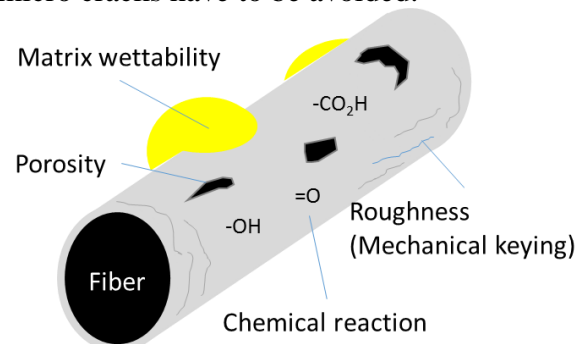

Figure 1. Fiber surface characteristics

A lot of testing methods for evaluating t_o have been proposed such as single fiber fragmentation test (SFFT) [10], push out

test [11], pull out test [12], dan micro bond test [13]. Among those testing methods, SFFT is known as a common method used for evaluating t_o. Compared with other methods, SFFT is considered relatively easy to be conducted. SFFT also produces actual stress transfer between fiber and matrix of a real structural composite condition. However, the SFFT usually provides high variation of t_o value even for the same testing procedure and the same type of specimen [14].

In this paper, the procedure of SFFT is reviewed. Firstly, t_o evaluation using SFFT is demonstrated. Two types of SFFT specimens, which are the specimen with agent-material and without agent-material of an interface, were manufactured. The shear stress on interface was analyzed by using Kelly-Tyson model [10]. From testing results, potential errors on SFFT method caused by simplification of model analysis are comprehensively discussed. Moreover, several proposed improvements with modifying the method and its analysis are also demonstrated.

Single Fiber Fragmentation Test

Specimen preparation. SFFT specimens must be manufactured with high dimensional accuracy in order to assure reliable testing results. Figure 2 shows manufacturing process of the specimens. After determining the specimen dimension, a positive aluminum mold was created. Note that specimen cross section (2 x 2 mm) had to be created with small tolerance. High precision CNC machine can be used to create the positive mold. Further, a negative mold made by silicon rubber liquid was created by using positive mold. After waiting for 1 day, the silicon rubber became solid and ready to be used for creating specimen.

The specimens used in this paper was made by single carbon fiber produced by TOHO Tenax Co. Ltd., and epoxy produced by Konishi chemical Co. Ltd. Two types of

specimens were manufactured with different fiber surface treatment. For the first specimen, the carbon fiber received from manufacturer was used directly. This means the fiber surface still contained some agent-material. Meanwhile, the carbon fiber for the second specimen was conditioned beforehand by soaking it into acetone for 5 hours and rinsed by water. This treatment was conducted to remove the agent-material on the carbon fiber surface, thus making the second specimens did not contain any agent-material.

Epoxy was inserted in negative mold followed by single carbon fiber. The tip of carbon fiber was imposed by a load in order to keep the fiber in straight position when the epoxy shrunk during the curing time. After 7 days, the specimens were taken from the negative mold. A top surface of the specimen was gradually polished by using sand papers of P600, P2000, SC800/2400, and SC1200/4000 until the thickness of specimen reached 2 mm. Moreover, to increase transparency, the surface specimens were painted by silicon oil. The specimens were then checked using microscope. Only the specimen with clearly seen and straight carbon fiber was used for the tests.

Testing method. The created specimens were then tested by using micro-tensile testing machine. The testing applied tensile speed of 0.0067 mm/minute. Low speed was used to avoid viscoelastic behavior of epoxy and ease detection of crack position. Figure 3a shows schematic tensile test of the specimen. On initial condition, carbon fiber was still perfectly connected. If a tensile force (F) was increased, the fiber would have cracks and formed a lot of fragments. The fiber cracks occurred because the fiber stiffness was higher than matrix stiffness. The fiber fragment disconnected continuously as long as length of fiber fragment (L) was longer than critical length of the fragment (L_c). On certain F, a new fragment would not form again even though F was increased. This

condition is called saturated condition in which all L is shorter than L_c. The L distribution in saturated condition follows Eq. 1.

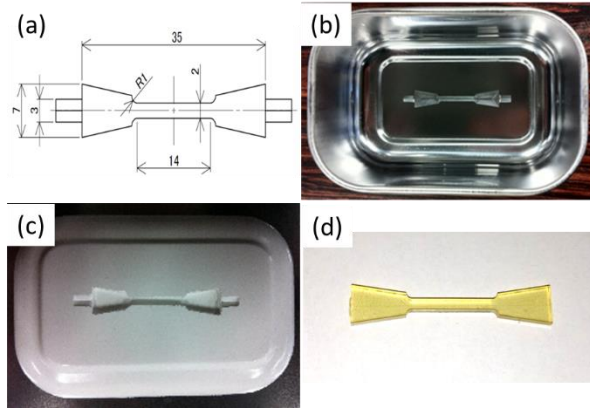$$\frac{L_c}{2} < L \leq L_c \qquad (1)$$

Figure 2. (a) specimen dimension (unit: mm), (b) positive mold, (c) negative mold, and (d) specimen

Furthermore, by using normal distribution approach for L, the relationship between an average length of fiber fragment ($\bar{L}$) and L_c can be formulated as follows,

$$\bar{L} = \frac{\sum_{i=1}^{N} L_i}{N} = \frac{3}{4} L_c \qquad (2)$$

where N is a number of fiber fragment.

Figure 3b shows stress distributions in the fiber of initial and saturated conditions. On the crack position, the fiber stress is zero. Kelly-Tyson modeled stress on a fiber fragment in one dimension as shown in Figure 3c. The fiber stress distribution (σ_z^f) and shear stress in the interface (t_s) can be seen in the Figure. The relationship between fiber strength (σ_{uts}^f) and t_o can be formulated as follow,

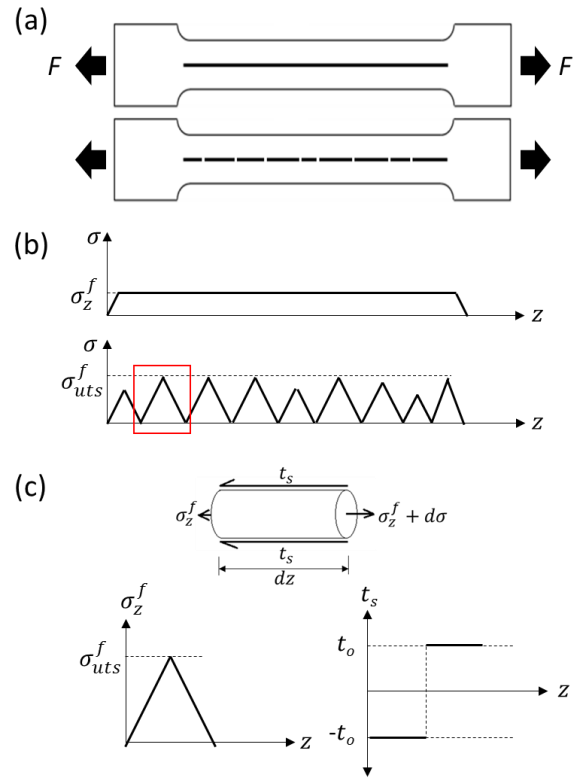$$t_o = \frac{\sigma_{uts}^f d}{2L_c} \qquad (3)$$

where d is fiber diameter.

Figure 3. (a) fragmentation process, (b) stress curve in fiber, and (c) Kelly-Tyson model

σ_{uts}^f can be calculated by recording a strain (ε_a) for each fiber crack. The fiber crack density (n) can follow a power function as shown in Eq. 4.

$$n = \frac{1}{L_o}\left(\frac{\sigma_z^f}{\sigma_0}\right)^m = \frac{1}{L_o}\left(\frac{E_f \varepsilon_a}{\sigma_0}\right)^m \qquad (4)$$

where E_f is elastic modulus of carbon fiber, σ_o is characteristic stress, L_o is length of measured area, and m is Weibull modulus. σ_o and L_o can be determined from n - ε_a curve obtained from the testing. Further, σ_{uts}^f is finally calculated by using Eq. 5.

$$\sigma_{uts}^f = \sigma_0 \left(\frac{L_o}{L_c}\right)^{1/m} \qquad (5)$$

Crack detection. For obtaining n - ε_a curve, L distribution, and $\bar{L}$, crack position and ε_a when the crack occurred have to be observed and recorded carefully. Figure 4 shows diagram of micro-tensile test

machine used for SFFT. The photoelastic apparatus was installed for detecting fiber crack positions. The apparatus consisted of polychromatic light source, polarizer, analyzer, microscope, camera, and computer for data recording. A specimen was positioned between polarizer and analyzer. The polarizer orientation was parallel to fiber orientation and load direction whereas analyzer orientation was perpendicular to them. These orientations produced dark figure at initial condition because the polychromatic light would be perfectly filtered by polarizer and analyzer.
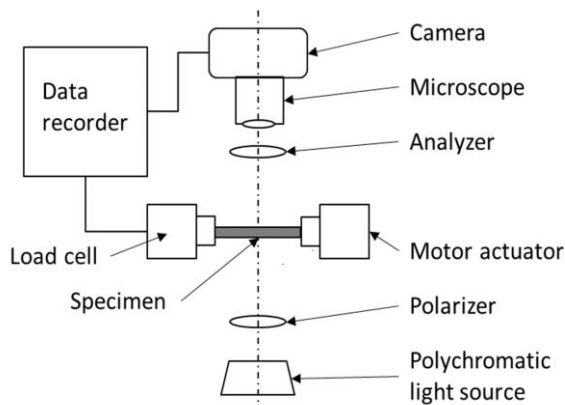

Figure 4. Diagram of micro tensile test with photoelastic apparatus

For detecting fiber crack by using photoelastic concept, matrix of the specimen have to be transparent and have temporal birefringent behavior i.e. a material which have two refractive indexes if F is imposed. Most of polymers for example, epoxy, have this behavior. These refractive indexes represent maximum and minimum principal stress difference in matrix and cause light interference so that the light can be captured by the camera when a fiber crack occurs. It is noted that isoclinic phenomenon, a condition when principal stress orientation equals to polarizer orientation, can appear, which causes dark condition remain occurs. Therefore, only light around fiber crack region, which the principal stress orientation is different with polarizer orientation due to shear stress, can be captured by the camera. Furthermore, ε_a can be calculated and recorded from load cell.

Results and Discussion

Interfacial strength. Figure 5a and 5b shows initial and saturated conditions of specimens which are captured by camera. By increasing microscope magnification, the fiber crack position and L can be clearly seen (see Figure 5c). The light indicates stress concentration in the matrix around the interface can be seen. There is also dark region on the tip of fiber crack that indicates debonding interface occurs along L_d.

Figure 6a and 6b show curve to ε_a for specimens with agent-material and without agent-material. From this curve, m parameter and σ_o in Eq. 4 can be determined. Table 1 and 2 show parameters obtained from the curve of each specimen. It is noted that used E_f is 240 GPa, which is based on TOHO Tenax datasheet. In saturated condition, L is then measured and plotted as shown in Figure 7. From the Figure, $\bar{L}$ of specimen with agent-material is shorter than that of without agent-material. The short $\bar{L}$ indicates strong interfacial bonding and vice versa.

Table 1. m and σ_o for specimen with agent-material

No.	Specimen	m (-)	σ_o (MPa)
1	Specimen 1	10.27	3354.5
2	Specimen 2	7.09	3299.8
3	Specimen 3	8.26	3635.7
4	Specimen 4	8.96	3217.3

Table 2. m and σ_o for specimen without agent-material

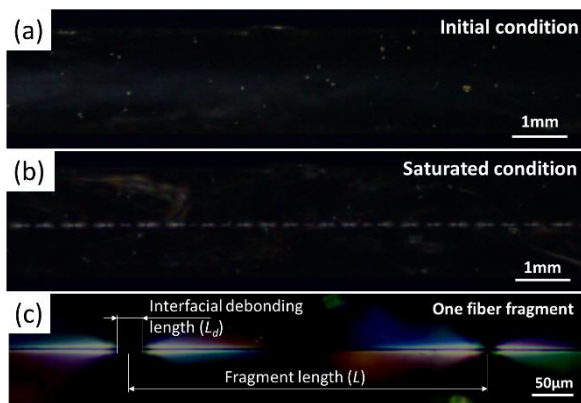| No.	Specimen	m (-)	σ_o (MPa)
1	Specimen 1	29.35	3622.2
2	Specimen 2	24.08	3766.4
3	Specimen 3	12.14	3637.2

Figure 5. (a) initial condition and (b) saturated condition of fragmentation, and (c) measurement of fragment length
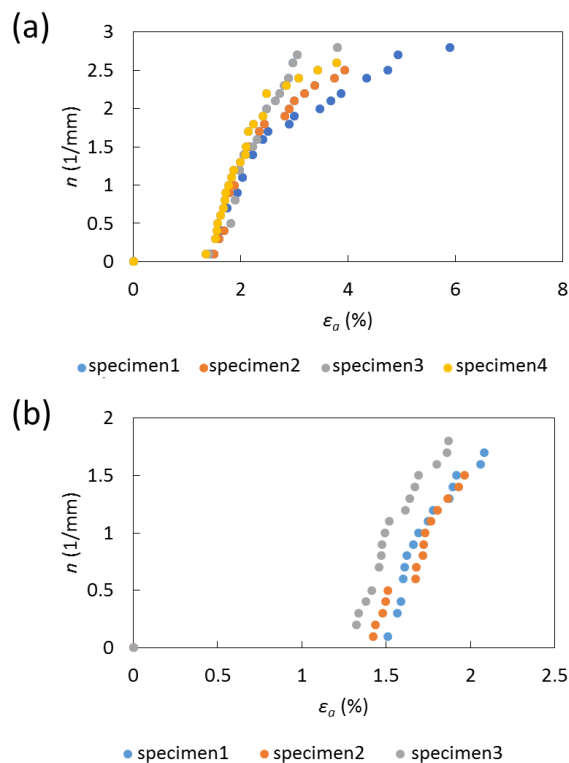

Figure 6. Fiber crack density to strain for (a) specimen with agent-material and (b) specimen without agent-material

L distribution of the specimen with agent-material seems narrower than conditioned specimen. This result indicates that the slip condition in the interface in which the interfacial debonding appears without fiber crack initiation might occur when the interfacial bonding is weak. This condition is proven by calculating L_c using

Eq. 2. According to Eq. 1, L should not be over the L_c value, which is calculated by using Eq. 2. However, on several specimens especially the conditioned specimens, there are fiber fragments which are longer than L_c. It means potential slip condition in the interface has happened.

Furthermore, by using Eq. 3 and 5, σ^f_{uts} and t_o can be obtained and plotted on Figure 8a. σ^f_{uts} showed decreasing on conditioned specimen. It occurs because the bonding layer of the interface is not only used for strengthening the interface but also for increasing σ^f_{uts}. On Figure 8b, t_o shows decreasing almost 50% for conditioned specimen. It is noted that mechanical keying caused by the roughness of fiber surface give a prominent contribution to t_o value on the conditioned specimen case. This means the mechanical keying significantly contribute to t_o value particularly for shear mode crack.

From testing results with two types of specimens, SFFT can differentiate a quality of interfacial bonding. The spread of testing results of around 20% also shows that SFFT is reliable to be used for evaluating t_o. This issue is important particularly in evaluating the effectiveness of adhesive layer of interface on fiber manufacturing industries.

Improvement of Method. Although SFFT can differentiate t_o for two types of specimens with different treatment qualitatively, SFFT actually still has problem of accuracy. The testing accuracy i.e. the true value of t_o is still arguable. There are several reasons as follows;

- Kelly-Tyson model that is usually used on the SFFT is too simple because it does not consider interfacial debonding phenomenon.
- In analyzing SFFT, the saturated condition of fiber cracks is required whereas this condition always occurs on the range of plastic deformation of matrix. For the matrices having low ultimate tensile strain, the saturated condition might not occur.

- On SFFT analysis, slip condition is not considered although it is possible especially on low t_o.
- The effects of interfacial stiffness are not considered on the SFFT analysis. Most of the models assume rigid condition for the interface [15].
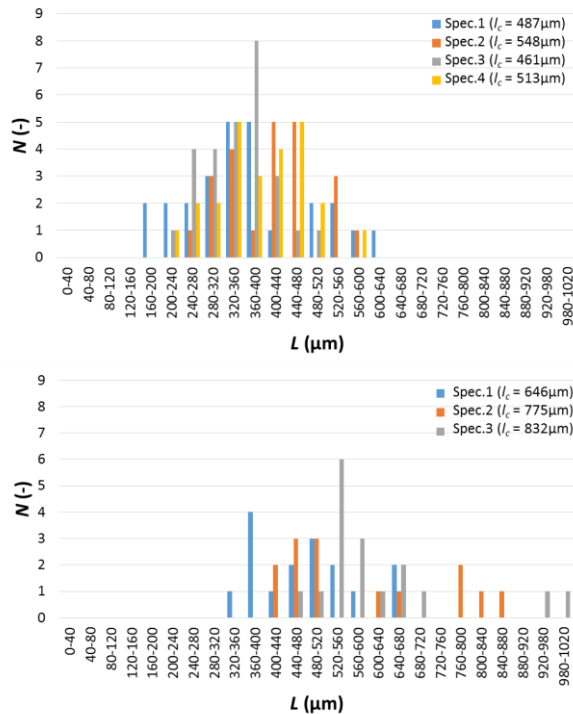

Figure 7. Fragment length distribution for (a) specimen with agent-material and (b) without agent-material
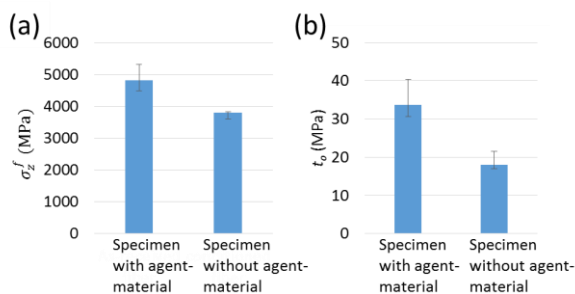

Figure 8. (a) fiber strength and (b) Interfacial strength

From explained problems, there are a lot of improvements proposed by researchers in order to increase the testing accuracy. For example, Kim et al. defined shear strength parameter for considering debonding process and friction after debonding in the interface [16]. Wagner et al. proposed a model based on energy balance and defined interfacial toughness [17]. Kimura et al. refined Wagner model by considering plastic deformation near the interface [18]. On the recent researches, interfacial crack is always explained by using cohesive zone mode [19]. This model has been proposed by many researchers such as Nishikawa et al. [20], Ma-Kishimoto [21], Willam et al., [22] dan Budiman et al. [23]. The cohesive zone model based on traction-separation law is believed as ideal model for explaining interfacial crack.

For applying cohesive zone model, a direct observation of stress around the interface is required. The stress, which has relationship with t_o, can be observed by modifying photoelastic apparatus [24-26]. An analysis using image processing technique is also required in order to assure clear stress observation [27].

It has to be emphasized, even though there are a lot of improvements have been proposed, SFFT still becomes basic testing for obtaining t_o. Most of the modifications are focused on proposing models and their better analyses for obtaining more accurate results. However, the basic concept of SFFT is still used due to its advantages.

Conclusion

SFFT as a method to evaluate t_o has been reviewed in this paper. From two types of specimens with different fiber surface treatment, SFFT has ability to evaluate the quality of interface properly. However, this method still has to be modified further for better accuracy. The main problems of SFFT are comprehensively discussed in this paper including examples of proposed improvement. Furthermore, standardization of SFFT method is urgently required to provide a uniform analysis so that the results can be compared quantitatively.

Reference

[1] M.J. Hinton, P.D. Soden, Predicting failure in composite laminates: the background to the exercise, Compos. Sci. Tech. 58 (1998) 1001-1010.

[2] M.J. Hinton, A.S. Kaddour, P.D. Failure criteria in fibre-reinforced-polymer composites: The world-wide failure exercise, first ed., Elsevier, 2004.

[3] J. Wang and W. K. Chiu, "Prediction of matrix failure in fibre reinforced polymer composites," J. Eng., vol. 2013, Article ID 973026, 9 pages, 2013.

[4] S.K. Ha, K.K. Jin, Y. Huang, Micromechanics of failure (MMF) for continuous fiber reinforced composites, J. Compos. Mater. 42 (2008) 1873-1895.

[5] L.J. Broutman, B.D. Agarwal, Effect of the interface on the mechanical properties of composites. Rheol. Acta. 13 (1974) 618-626.

[6] M. Sharma, S. Gao, E. Mader, H. Sharma, L.Y. Wei, J. Bijwe, Carbon fiber surfaces and composite interphases, Compos. Sci. tech. 102 (2014) 35-50.

[7] Z. Dai, F. Shi, B. Zhang, M. Li, Z. Zhang. Effect of sizing of carbon fiber surface properties and fiber/epoxy interfacial adhesion. Appl. Surf. Sci. 257 (2011) 6980-6985.

[8] J. K. Kocsis, H. Mahmood, A. Pegoretti, Recent advance in fiber/matrix interphase engineering for polymer composites, prog. Mater. Sci. 73 (2015) 1-43.

[9] Q. Wu, M. Li, Y. Gu, S. Wang, L. Yao, Z. Zhang, Effect of sizing on interfacial adhesion of commercial high strength carbon fiber-reinforced resin composites, Polym. Composites 37 (2016) 254-261.

[10] A. Kelly and W. R Tyson, Tensile properties of fibre-reinforced metals: copper/tungsten and copper/molybdenum, J. Mech. Phys. Solids 13 (1965) 329-350.

[11] J.H. You, W. Lutz, H. Gerger, A. Siddiq, A. Brendel, C. Hoschen, S. Smauder, Fiber push-out study of a copper matrix composite with an engineered interface: Experiments and cohesive element simulation, Int. J. Solids Struct. 46 (2009) 4277-4286.

[12] W.C. Choi, S.J. Jang, H.D. Yun, Interface bond characterization between fiber and cementitious matrix, Int. J, Polym. Sci., vol. 2015, Article ID 616949, 11 pages, 2013.

[13] M. Nishikawa, T. Okabe, K. Hemmi, N. Takeda, Micromechanical modeling of the microbond test to quantify the interfacial properties of fiber-reinforced composites, Int. J. Solids Struct. 45 (2008) 4098–4113.

[14] M.J. Rich, L.T. Drzal, D. Hunston, G. Holmes, W. Mcdonough, Round robin assessment of the single fiber fragmentation test, Proceedings of the American Society for Composites, 17th technical conference, Indiana, October 21-22, 2002.

[15] B.A. Budiman, K. Takahashi, K. Inaba, K. Kishimoto. The Influence of elastic bonding behavior at fiber-matrix interface to composite performance. Proceeding of the 11th International Conference on Durability Analysis of Composite Systems (DURACOSYS), Tokyo, September 15-17, 2014.

[16] J.K. Kim, L.M. Zhou, Y.W. Mai, Stress transfer in the fiber fragmentation test, Part I. An improved analysis based on shear strength criterion, J. Mater. Sci. 28 (1993) 6233-6245.

[17] H.D. Wagner, J.A. Nairn, M. Detassis, Toughness of interfaces from initial-matrix debonding in a single fiber composite fragmentation test, Appl. Compos. Mater. 2 (1995) 107-117.

[18] S. Kimura, J. Konayagi, H. Kawada, Evaluation of initiation of the interfacial debonding in single-fiber composites (Energy balance method considering an energy dissipation of the plastic deformation), JSME Inter. J. 49 (2006) 451-457.

[19] N. Chandra, H. Li, C. Shet, H. Ghonem, Some issues in the application of cohesive zone models for metal-ceramic

interfaces, Inter. J. Solids Struct. 39 (2002) 2827-2855.

[20] F. Ma, K. Kishimoto, A continuum interface debonding model and application to matrix cracking of composite. JSME Inter., 39A (1996) 496-507.

[21] M. Nishikawa, T. Okabe, N. Takeda, Determination of interface properties from experiments on the fragmentation process in single-fiber composites. Mater. Sci. Eng. A-Struct., 480 (2008) 549-557.

[22] K. Willam, I. Rhee, B. Shing, Interface damage model for thermomechancial degradation of heterogeneous materials, Comput. Method. Appl. M. 193 (2004) 3327-330.

[23] B.A. Budiman, K. Takahashi, K. Inaba, K. Kishimoto. A new method of evaluating interfacial properties of a fiber/matrix composite. J. Compos. Mater. 49 (2015) 465-475.

[24] B. Fiedler, K. Schulte, Photo elasticity analysis of fibre reinforced model composite materials, Compos. Sci. Technol. 57 (1997) 859-867.

[25] F.M. Zhao, E.A. Patterson, F.R. Jones. Phase-stepping photoelasticity for quantifying the interfacial response in fiber composites at fibre-breaks. Mater. Sci. Eng. 410 (2005) 83-87.

[26] F.M. Zhao, R.D.S. Martin, S.A. Hayes, E.A. Patterson, R.J. Young, F.R. Jones, Photoelastic analysis of matrix stresses around a high modulus sapphire fiber by means of phase-stepping automated polariscope, Compos. Part A-Appl. S. 36 (2005) 229-244.

[27] T.H. Baek, M.S. Kim, D.P. Hong. Fringe analysis for photoelasticity using image processing techniques. Inter. J. Softw. Eng. and Appl. 8 (2014) 91-102.